Materials Science & Engineering A 737 (2018) 105–114

Contents lists available at ScienceDirect

Materials Science & Engineering A

journal homepage: www.elsevier.com/locate/msea

Plastic deformation dominates chemical reactions in Ti/Si multilayered nanofilms

Hiroyuki Hirakata[a,*], Takashi Kawai[b], Toshiyuki Kondo[b], Kohji Minoshima[b]

[a] Department of Mechanical Engineering and Science, Kyoto University, Kyoto-daigaku-Katsura, Nishikyo-ku, Kyoto 615-8540, Japan
[b] Department of Mechanical Engineering, Osaka University, 2-1 Yamadaoka, Suita, Osaka 565-0871, Japan

ARTICLE INFO

Keywords:
Chemical reaction
Multilayered nanofilms
Stress
Plastic deformation
Titanium
Silicon
Silicide

ABSTRACT

The purpose of the study was to clarify the exothermic chemical reaction mechanisms in Ti/Si multilayered nanofilms under mechanical loading. We conducted in situ compression experiments of truncated-cone specimens of polycrystalline-Ti/amorphous-Si multilayered nanofilms (bilayer thickness of ~ 34 nm) deposited by electron beam evaporation within a scanning electron microscope. The true stress increased almost linearly with increasing true strain and the tangent modulus began to decrease at ~ 3 GPa. Transmission electron microscopy of the deformed specimens confirmed that each layer was plastically compressed in the stacking direction and expanded in the in-plane direction, resulting in an increase in the Ti/Si interface area. Selected-area electron diffraction analysis revealed that a new crystal structure, proposed to be Ti_5Si_4 and/or TiSi, was generated on the Ti/Si interface and within the Ti layer. In addition, the volume of the specimens decreased with increasing strain, supporting the hypothesis of a chemical reaction occurring. The chemical reaction was induced at the new reactive Ti/Si interface by the partial fracture of preexisting compound layers due to tensile stresses in the in-plane direction, and/or induced by diffusion-induced mixing through the thinned compound layers. These findings present the possibility of controlling the chemical reaction by local mechanical loading. The observed exothermic reaction can be used for various applications, such as local heating in large-scale micro- and nanodevices.

1. Introduction

When sufficient energy is supplied to a localized region of multilayered nanofilms composed of alternating layers with thicknesses of the order of 10 nm, the constituent elements react with each other and release heat. This exothermic reaction results in generation of new compounds in this region, and the generated heat diffuses to adjacent unreacted regions. If the temperature in the neighboring regions becomes high enough to promote additional reactions, a self-sustained propagating reaction (SPR) occurs [1–4]. SPR behavior has been reported in nanofilms composed of combinations of metal/metal, metal/semiconductor, metal/metalloid, and metal/metal-oxide; for example, aluminides (e.g., Al/Ni), silicides (e.g., Ti/Si), borides, carbides, zirconides, and bi-metals [4]. This reaction has a high propagation speed (0.1–100 m/s) in multilayered nanofilms with a total thickness of several micrometers and generates heat only in the region near the nanofilms; hence, it can be applied in joining technology, ignition devices, and power sources for micro- and nanodevices, while limiting thermal damage to the surrounding regions [4,5].

SPR is induced not only by electrostatic discharge, electrical heating, and laser irradiation, but also by mechanical impact by a sharp tipped stylus [1,2,6,7]. SPR by mechanical impact is a two-step process: (i) Initial reaction by mechanical loading; and (ii) ignition and propagation of a reaction wave. Many studies have been conducted on SPR properties, such as the ignition threshold and the propagation speed [3,4,7]; the ignition threshold is commonly characterized by the ignition temperature or energy density. The ignition threshold increases and the propagation speed decreases with increasing thickness of the bilayer film and intermixed layer between the two layer materials at the interface [7] due to a lower rate of interdiffusion as the mass diffusion length increases with increasing bilayer thickness. In addition, the presence of premixed layers reduces the amount of stored chemical energy. However, detailed mechanisms regarding the initial chemical reaction due to mechanical loading are still unclear. This chemical reaction occurs at a temperature well below the melting point and eutectic temperature, implying that it is a solid-state reaction [7]. Solid-state atomic mixing can be induced by diffusion or plastic deformation. Since the reaction occurs in a very short time while diffusion occurs

* Corresponding author.
E-mail address: hirakata@me.kyoto-u.ac.jp (H. Hirakata).

https://doi.org/10.1016/j.msea.2018.09.031
Received 5 August 2018; Accepted 11 September 2018
Available online 12 September 2018
0921-5093/

over a longer time scale, we focused on the role of plastic deformation.

The purpose of the study was to clarify the mechanisms of the initial chemical reaction of Ti/Si multilayered nanofilms subjected to mechanical loading. Due to the structural anisotropy of the multilayered nanofilms, the deformation mechanism depends on the loading mode with respect to the stacking direction. Here, we focus on the deformation and chemical reaction under compression loading in the stacking direction as a basic mode. We fabricated truncated-cone-shaped specimens using the focused ion beam (FIB) method from polycrystalline-Ti/amorphous-Si multilayered nanofilms (bilayer thickness of ~ 34 nm) deposited by electron beam evaporation, and then conducted compression experiments under in situ field emission scanning electron microscopy (FESEM). We evaluated the chemical reaction via the change in the crystal structure using transmission electron microscopy (TEM) and selected-area electron diffraction (SAD).

2. Experimental method

2.1. Materials

In order to fabricate Ti/Si multilayered nanofilms with a stoichiometric ratio of Ti:Si = 5:4, where the compound Ti_5Si_4 has a large standard enthalpy of formation −81 kJ/mol [8], the target thicknesses of Ti and Si were set to 15.7 nm and 14.3 nm, respectively, to achieve a bilayer thickness of 30 nm. A Ti/Si multilayered sample with 62 bilayers was prepared by alternately depositing Ti (purity 99.9%) and Si (purity 99.9999%) on a Si (001) substrate using electron beam evaporation (Eiko Engineering Co., Ltd.). The base pressure was 2.1×10^{-5} Pa, the deposition pressure was $< 3.2 \times 10^{-4}$ Pa, and the deposition rate was ~ 0.1 nm/s for both Ti and Si during deposition.

TEM samples with a thickness of ~ 100 nm were prepared from the Ti/Si multilayered nanofilms using FIB in a FIB/FESEM dual-beam instrument (Thermo Fisher Scientific, Varsa 3D). To suppress surface damage during FIB, a Pt layer was first deposited on the sample surface by electron beam induced deposition. A TEM (Hitachi High-Technologies Corporation, H-800) was used for low-magnification observation and a field-emission TEM (Hitachi High-Technologies Corporation, HF-2000) was used for high-resolution (HR) observation. In both cases, the acceleration voltage was set to 200 kV. TEM and HR-TEM images of the sample are shown in Fig. 1(a) and (b), respectively. Fig. 1(a) clearly shows the multilayer structure of Ti (dark areas) and Si (light areas), from which a bilayer thickness of ~ 34 nm was measured, which was slightly thicker than the target value of 30 nm. Fig. 1(b) confirmed that the Ti layer had a polycrystalline structure (thought to be α-Ti), while the Si layer was amorphous [6].

2.2. Compression experiments

Micrometer-sized truncated cone specimens were fabricated using FIB from the Ti/Si multilayered nanofilms. Fig. 2(a) and (b) show FESEM images of a representative specimen. The front view image (Fig. 2(b)) shows that the edges of the specimens were rounded. The height h, diameters of the upper and lower parts, d_u and d_l, respectively, and the radii of curvature ρ_{ur}, ρ_{ul}, ρ_{lr}, and ρ_{ll} of the specimen are defined as indicated in Fig. 2(b). Table 1 shows the dimensions measured from FESEM images, which are the average value and standard deviation of five specimens (four were used for compression experiments and one was used as the control sample for observing the undeformed state).

As illustrated in Fig. 2(c), compression experiments were conducted using an FIB-fabricated diamond flat punch. A mechanical loading system (Hysitron, Inc., Picoindenter PI-85) with a rated force of 10 mN and rated displacement of 5 μm was used, where the load P was electrostatically applied and the displacement u was measured by a capacitance sensor. All experiments were conducted under in situ FESEM (JEOL Ltd., JSM-7001F) observation at room temperature (~ 293 K) under vacuum (pressure $< 9.6 \times 10^{-5}$ Pa).

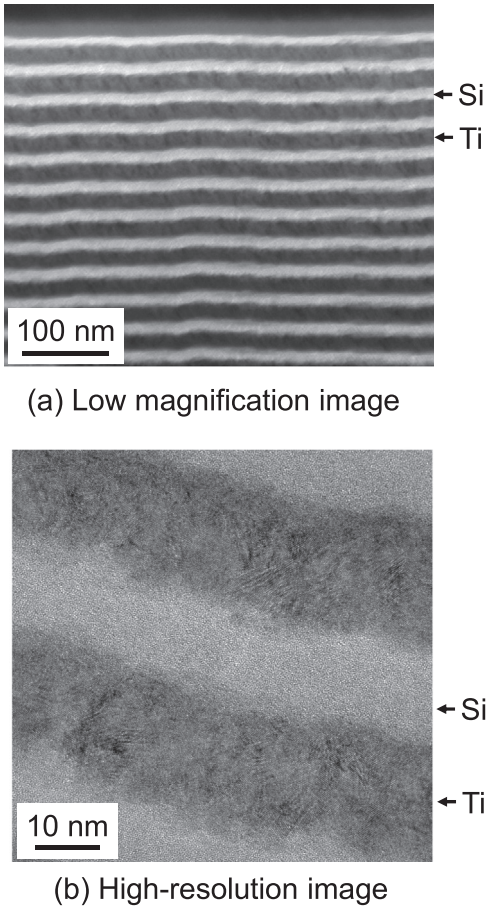

Fig. 1. TEM micrographs of Ti/Si multilayered films.

The experiments were performed under closed-loop displacement control; the displacement was increased at a constant rate of 10 nm/s, held at the maximum displacement for 10 s, and then decreased at a rate of −10 nm/s. The maximum displacement for specimens u400-1 and u400-2 was 400 nm, while that of the other two specimens (u600-1 and u600-2) was 600 nm.

2.3. Evaluation of chemical reactions using TEM

In order to investigate whether a chemical reaction was induced by mechanical loading, a specimen not subjected to mechanical loading (control specimen) was compared to u400-1 and u600-1 (maximum displacements of 400 nm and 600 nm, respectively) after compression experiments. The samples were observed by TEM and the SAD patterns were analyzed. TEM samples were prepared from the central region of the truncated-cone specimens as described in Section 2.1.

3. Results

3.1. Compression behavior

Fig. 3 shows P–u curves for all compression experiments; the scatter of the data was small, indicating good reproducibility. It can be seen that P monotonically increased with increasing u, and permanent deformation remained after unloading. The amount of the permanent deformation was ~330 nm for the specimens with maximum displacement of 400 nm and ~510 nm for the specimens with maximum displacement of 600 nm. FESEM images before and after compression are shown in Fig. 4. The height of the specimens decreased and the diameter increased because of compression. In the u600 specimens, cracks